Polymer Trace Devolatilization: II. Case Study and Experimental Verification

Chi-Tai Yang and Theodore G. Smith
Dept. of Chemical Engineering, University of Maryland, College Park, MD 20742

David I. Bigio
Dept. of Mechanical Engineering, University of Maryland, College Park, MD 20742

Colin Anolick
Central Research and Development Dept., DuPont, Experimental Station, Wilmington, DE 19880

In this work, the bimodal/film model is compared with the cell model based on a case study using polystyrene/styrene devolatilization. It shows improvements over the cell model: (1) it requires a lower initial number of bubbles, which is more physically realistic and (2) it takes into account the observation of a limiting foam volume growth for a specific polymer in devolatilization. A stripper dispersion experiment was designed to investigate the effect of dispersed nitrogen stripper bubbles on the foam dynamics and devolatilization efficiency. The variables examined include polymer viscosity, initial volatile concentration, and the initial number and size of dispersed stripper bubbles. Polymer viscosity was the dominant factor in limiting the maximum foam volume expansion. The number and size of dispersed stripper bubbles show positive and negative effects (which are only secondary) on the maximum foam volume expansion, respectively. The initial volatile concentration has no effect on limiting the maximum foam volume expansion.

Introduction

In Part I, we developed a mathematical model for foam devolatilization. The model combines a bimodal model for foam growth with a film model for devolatilization. The bimodal model describes the initial formation and growth of the volatile and stripper bubbles. When foaming and breakup occur at some critical foam-volume growth, the film model is used to complete the devolatilization by mass diffusion of the volatile component through the polymer films into the contiguous gas phase. In the current study, we compare the bimodal/film model with the cell model based on a case study on polystyrene/styrene devolatilization in a Werner & Pfleiderer (W & P) ZSK-90 corotating twin-screw extruder (Werner, 1980). In this article, we also examine experimentally the effect of dispersed stripper bubbles in polymer devolatilization, and compare the bimodal/film model with the experimental results. It has been previously reported that there is a limiting maximum foam-volume expansion for a specific polymer (Yang et al., 1996a,b, 1997). Although the factors in limiting the maximum foam-volume change are not clear, polymer viscosity could be one of the main factors. Thus in this work we are also interested in the effect of polymer viscosity in limiting the maximum foam-volume expansion. In summary, the objectives of this study are:

- To compare the bimodal/film model with the cell model
- To compare the bimodal/film with experimental results
- To study the effects of the process conditions (polymer viscosity and volatile concentration) and the characterization of a stripping agent (the initial number and size of nitrogen bubbles) on the maximum foam-volume expansion and the thermodynamic devolatilization efficiency.

Correspondence concerning this article should be addressed to D. I. Bigio.
Current address of C.-T. Yang: Formosa Plastics Corporation, P.O. Box 320, Delaware City, DE 19706.

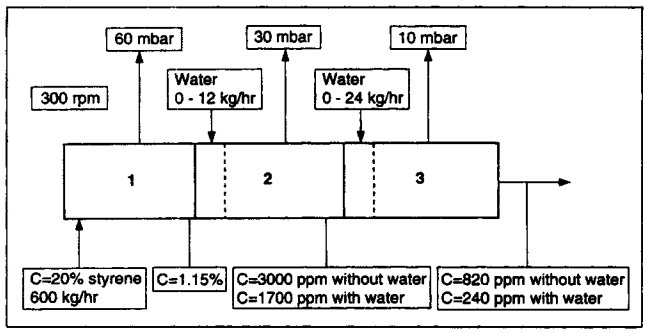

Figure 1. Polystyrene/styrene devolatilization in a ZSK-90 corotating twin-screw extruder (Werner, 1980).

Case Study: Polystyrene/Styrene Devolatilization

This section demonstrates the use of the bimodal/film model and the cell model in describing the performance of foam devolatilization (Yang et al., 1996a). Devolatilization of styrene monomer from polystyrene in a W&P ZSK-90 corotating twin-screw extruder is used as a case study (Werner, 1980).

Figure 1 shows the simplified diagram and operating conditions of the ZSK-90 corotating twin-screw extruder for devolatilizing a polystyrene solution containing 20 wt. % styrene monomer in three vacuum stages to a residual monomer concentration of 240 ppm. We use the devolatilization results in the second vacuum section for illustration. Two wt. % of water is injected into the extruder before the second vacuum section as a stripping agent to enhance devolatilization performance by reducing the styrene concentration from 1.15 wt. % to 1,700 ppm, as compared to 3,000 ppm without the addition of water. The operating conditions and materials properties are listed in Tables 1 and 2. Several studies in the literature reported that polystyrene melt can foam under the following initial styrene concentrations and vacuum pressures: 2,300 ppm and 0.8 mmHg (0.1 kPa) (Albalak et al., 1987); 10,000 ppm and 1 to 3 mmHg (0.4 kPa) (Albalak et al., 1990); 3,000 ppm and 50 mmHg (7 kPa) (Tukachinsky et al., 1993); and 6,000 ppm and 3 mmHg (0.4 kPa) (Tukachinsky et al., 1994). The conditions at the second vent section in this case

Table 1. Operating Conditions for the Polystyrene/Styrene Devolatilization in the Second Vacuum Section in a ZSK-90 Corotating Twin-Screw Extruder

Conditions	Values
Temperature (°C)	250
Vacuum (mbar)	30
Screw speed (rpm)	300
Throughput (kg/h)	600
Degree of fill (%)	16.5
Average residence time (s)	4
Water stripping agent (wt. %)	0/2.0
Inlet monomer concentration (ppm)	11,500
Outlet monomer concentration (ppm)	3,000/1,700*
Equilibrium monomer concentration (ppm)	974/81*
Final monomer concentration (ppm)	3,000/1,700*
Thermodynamic devolatilization efficiency (%)	80.75/85.82*

Source: Werner (1980).
*With addition of 2.0 wt. % water.

Table 2. Materials Properties of the Polystyrene/Styrene System at 250°C

Properties	Values
Diffusion coefficient*	4.07×10^{-6} cm^2/s
Henry's law constant **	34.8 atm
Melt density**	0.67 g/cm^3
Surface tension**	8.6 dyne/cm
Viscosity†	1,000 Pa·s

*Sakakibara et al. (1990).
**Lee and Biesenberger (1989).
†Newman and Simon (1980).

study should provide sufficient driving force for the polystyrene to foam. Since no data have been reported on the critical foam-volume expansion of polystyrene melt in the literature, it is assumed that polystyrene melt is able to expand to five times its initial volume before foam breakup.

In the numerical computation, the numbers of bubbles in the cell model and the bimodal/film model are adjustable parameters to be fit to the devolatilization results under the operating conditions.

Application of the models in predicting the thermodynamic devolatilization efficiency is shown in the following. Figure 2 shows the thermodynamic devolatilization efficiency and foam volume vs. time by using the cell model and the

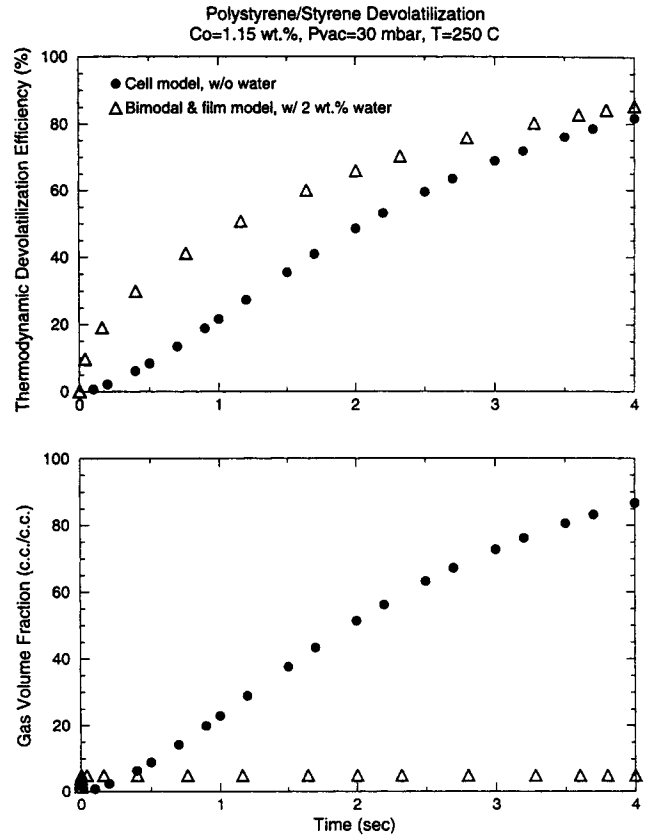

Figure 2. Computation results and comparison of models in describing polystyrene/styrene devolatilization.

For the cell model, $N_v = 2{,}000{,}000$ No./cm^3 liq. For the bimodal/film model, $N_v = 5{,}000$ No./cm^3 liq. and $N_s = 2{,}600$ No./cm^3 liq.

bimodal/film model for numerical simulation of devolatilization in the second vacuum section without and with the addition of water, respectively. The cell model requires a large number of volatile bubbles (2,000,000/cm^3 liq.) in order to satisfy the conditions. The free parameter is adjusted to force the model to predict the experimentally determined thermodynamic devolatilization efficiency. In the cell model for devolatilization as bubbles grow due to reduced ambient pressure and diffusion of the dissolved volatile from the polymer melt, the driving force for mass transfer decreases. The rate of devolatilization decreases as more volatile is removed from the polymer melt into the bubbles due to a reduction in the thermodynamic driving force. In addition, the operating conditions and materials properties suggest that the devolatilization process is diffusion-controlled. Therefore, a large number of bubbles is required to achieve a high degree of devolatilization in a short period of time. It is questionable whether such a high number of bubbles occurs in devolatilization. Newman and Simon (1980) studied polystyrene/styrene devolatilization in falling-strand-type equipment. They observed foaming of the polymer and estimated that bubble size was on the order of 1 mm. The number of bubbles was estimated on the order of 1,000/cm^3 liq.

Furthermore, using the initial number of bubbles for the cell model results in about 85 times the initial polymer volume at 4 s. It implies that the foam would have flooded the screw channel. A 16.5% degree of channel fill with polymer in the vacuum section can only accommodate a sixfold foam-volume expansion at most; otherwise, the foam may develop further downstream and plug the vacuum port. The high volume growth (85 times) further validates the poor assumption in the cell model that "devolatilization" is considered as the volatile diffuses from the polymer melt into the growing bubbles. It is not applicable in extruder-based devolatilization processes in which the screw channels have a limiting volume. In addition, the shear flow in the rotating polymer pool may aid in foam breakup and limit the foam expansion.

The bimodal/film model is applied similarly to the same case. An initial number of 5,000 volatile bubbles is required to fit the data. By injecting 2 wt. % of water as the stripping agent, the partial vapor pressure of the styrene monomer is reduced from 30 mbar to 2.5 mbar. The dispersed stripper bubbles (2,600/cm^3 liq.) can expand the polymer to five times the initial volume very quickly. The film model is used to complete the computation at a very early stage of devolatilization. It is evident that not only does the thermodynamic devolatilization efficiency increase from 81% to 86%, but the rate of approach to the desired level of devolatilization increases as well.

From the preceding discussion, it is seen that a lower initial number of bubbles is needed in the bimodal/film model to fit to the experimental data. The number of bubbles used in the bimodal/film model is on the same order as that observed during devolatilization through the vacuum port. Although the number of 2,000,000 volatile bubbles used in the cell model could be calculated from the classic bubble nucleation theory, not all of the bubbles have the same driving force to grow and become visible during devolatilization. Furthermore, the cell model only considered the diffusion of the volatile component from the polymer into the bubbles as "devolatilization." This is only part of the complete picture of foam devolatilization. Devolatilization is completed only when the volatile in the bubbles diffuses through the polymer films into the contiguous gas phase and/or bubbles rupture to release the volatile to the contiguous gas phase. The other inadequacy in the cell model for devolatilization is clearly seen by the foam-volume fraction calculated. There is a limited amount of free volume in the screw channels of an extruder for foam growth and expansion. As shown in the foaming experiments, there is a constant maximum foam-volume expansion of a polymer. An 85 times foam-volume change calculated by the cell model did not explain the observation. Also, the 85 times foam-volume expansion requires that the extruder operate at less than 2% degree of channel fill in the vacuum section, which is not economically feasible.

Stripper Dispersion Experiment

This section reports on the design of a stripper-dispersion experiment to investigate the effect of dispersed nitrogen stripper bubbles on the foam dynamics and devolatilization results, and to compare it with the previously developed bimodal/film model (Yang et al., 1996b).

Materials

Low-molecular-weight polybutene was used as the model polymer in this experiment. Polybutenes of different viscosities at room temperature were used: 60, 90 and 200 Pa·s. The physical properties of the three types of polybutene are listed in Table 3 (Exxon, 1995; Amoco, 1995).

Carbon dioxide was used as the volatile component in this study. The solubility (or Henry's law constant) and diffusion coefficient of carbon dioxide in polybutene were determined by an independent conventional sorption experiment (Yang, 1995). This experiment is based on a simplified method of direct measurement of the volume of gas sorbed by a polymer specimen (Rosen, 1959). The diffusion coefficient is calculated based on a simple sorption and desorption kinetic model (Crank and Park, 1968). The diffusion coefficient and solubility of carbon dioxide in polybutene are summarized in Table 4.

Nitrogen was used as the stripping agent. It was supplied from a gas cylinder at 15 psig (205 kPa) and was initially dispersed as bubbles into the polymer pool. The dispersion of nitrogen bubbles into the polymer pool is achieved through the use of fritted disks of different porous sizes.

Experimental system and procedure

Figure 3 is a diagram of the test chamber for the stripper-dispersion experiment. It is a glass tube with an inserted frit-

Table 3. Physical Properties of Polybutenes

Properties/Polybutenes	*PARAPOL* 1300	*INDOPOL* H300	*PARAPOL* 2400
Molecular Wt. (g/mol)*	1,300	1,330	2,350
Viscosity @ 100°F (cSt)*	27,230	—	143,900
Viscosity @ 25°C (Pa·s)**	60	90	200
Density @ 60°F (g/cm^3)†	0.895	0.902	0.907

*From product literature (Exxon, 1995; Amoco, 1995).
**Measured on a Rheometrics RFS II rheometer (Yang, 1995).
†Converted from product literature (Exxon, 1995; Amoco, 1995).

Table 4. Diffusion Coefficient and Solubility of Carbon Dioxide in Polybutene at 25°C

Properties/Polybutenes	*PARAPOL* 1300	*INDOPOL* H300	*PARAPOL* 2400
D (cm^2/s)	9.0×10^{-7}	7.1×10^{-7}	3.4×10^{-7}
S (cm^3@STP/$cm^3\cdot atm$)	1.9	1.5	1.1
H_w (atm)	240	306	420

Source: Yang (1995).

ted disk. First, the polybutene sample was transferred into the chamber. Vacuum was applied to degass the system. Carbon dioxide was introduced until the system reached the determined gas pressure. When the experiment began, the pressurizing of carbon dioxide was stopped and nitrogen was injected from the bottom of the fritted disk. This flow of nitrogen gas through the porous fritted disk dispersed in the polybutene as bubbles. The initial number and size of dispersed nitrogen bubbles were photographed. Nitrogen gas left below the fritted disk was flushed by a partial vacuum. The desired vacuum level was then applied to the system for devolatilization. The glass trapping system used in the previous foaming experiment was used to collect desorbed carbon dioxide at a series of time intervals: 0–1, 1–3, 3–5, and 5–10 min (Yang et al., 1996b). The whole experimental process was videotaped for later study. Carbon dioxide vapor pressure in the glass traps was measured by the P-V-T method (Yang, 1995).

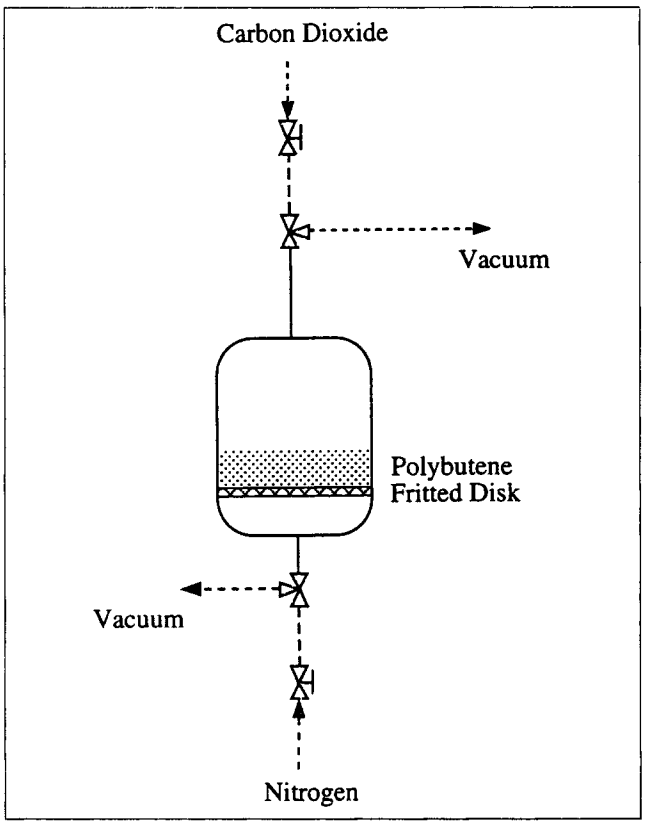

Figure 3. Apparatus for stripper dispersion experiment.

Experimental conditions and process parameters

The variables examined in this experiment include:

- Viscosity of polybutene: 60, 90, and 200 Pa·s;
- Initial carbon dioxide concentration: 60 and 30 psig;
- Initial number and size of nitrogen bubbles.

Nitrogen bubbles were introduced into the polymer pool by forcing nitrogen gas through the porous fritted disk from the bottom of the test chamber. Two porous sizes of fritted disks were used: 10–15 μm and 170–220 μm.

We photographed the initially dispersed nitrogen bubbles in the polybutene pool, taking two to four views of each experimental condition. Black-and-white prints were made for further image processing and analysis in order to determine the number and size distribution of the nitrogen bubbles.

The whole experimental process was videotaped to monitor foam height as a function of time. Visual observation establishes the relationship between the foam volume growth and process parameters.

Image analysis

The number and size distribution of dispersed nitrogen bubbles were determined by semiautomatic digital image processing and analysis software. Image 1.44, a public domain program developed by the National Institutes of Health (NIH), was employed for bubble population analysis.

First, the black-and-white prints were scanned and converted into the digitized image files. The digitized image was analyzed by the NIH Image 1.44 program. A representative number of bubbles in each image was selected. Two to four fields of view for each experimental condition were used. Although the nitrogen bubbles looked nearly spherical, the maximum and minimum diameters of the selected bubbles were measured. The equivalent diameter of a spherical bubble is calculated as:

$$d_i = (a \times b \times b)^{1/3}, \tag{1}$$

where a and b are the maximum and minimum diameters, respectively, of the bubble measured from the image analysis.

The dispersion of nitrogen bubbles in polybutene is characterized by the number-averaged dispersed bubble diameter, d_n, and the volume-averaged diameter, d_v (or the moment mean diameter) by

$$d_n = \frac{\Sigma n_i d_i}{\Sigma n_i} \tag{2}$$

$$d_v = \left(\frac{\Sigma n_i d_i^3}{\Sigma n_i} \right)^{1/3}, \tag{3}$$

where d_i is the diameter of the spherical bubble, and n_i is its corresponding number. Note that large dispersed bubble-size distributions result in an average diameter value that overestimates the contribution of large bubbles. In our study, calculations have shown that the bubble-size distribution is sufficiently narrow: the polydispersity index $d_v/d_n \cong 1.0$–1.5. Therefore, we can use the number-averaged bubble diameter plus the standard deviation to give a range of bubble sizes in the dispersion process.

Table 5. Bubble Populations in the Stripper Dispersion Experiment with Polybutenes

Run No.	N_s (No./cm^3 liq.)	d_n (cm)	S.D. (cm)	ϕ_{max} (cm^3 gas/cm^3 liq.)
PARAPOL 1300/60 psig				
1	316	0.10957	0.03416	7.24
2	1,593	0.07558	0.01305	7.33
3	33	0.18024	0.05652	7.52
4	89	0.22044	0.04738	7.52
PARAPOL 1300/30 psig				
1	423	0.10716	0.08250	6.75
2	1,175	0.07122	0.01913	8.61
3	39	0.17030	0.05374	6.45
4	141	0.20296	0.08508	7.36
INDOPOL H300/60 psig				
1	248	0.09163	0.01993	4.96
2	1,043	0.07015	0.00782	5.15
3	24	0.25298	0.07785	3.41
4	113	0.17178	0.03991	4.46
INDOPOL H300/30 psig				
1	240	0.09261	0.01248	4.77
2	1,308	0.08360	0.01986	5.28
3	31	0.23090	0.06020	3.50
4	181	0.14672	0.03149	3.51
PARAPOL 2400/60 psig				
1	45	0.15650	0.06686	2.64
2	61	0.14838	0.08580	1.25
3	20	0.16515	0.10025	1.11
4	52	0.17848	0.06204	2.00
PARAPOL 2400/30 psig				
1	22	0.20460	0.08915	3.00
2	31	0.17229	0.10873	2.50
3	5	0.32611	0.13075	1.45
4	6	0.30026	0.09731	1.25

SI Conversion: kPa = psia × 6.895.

Experimental Observation

Four experiments were performed for each experimental condition. The variables in these four experiments are the initial number and sizes of the dispersed nitrogen bubbles in the polybutene samples. The sizes of the nitrogen bubbles are analyzed in the Image 1.44 software and summarized in Table 5. The maximum foam-volume expansions observed (ϕ_{max}) in the experiments are also listed. The initial number of bubbles was calculated by recognizing the initial bubble volume fraction from the experiment ($\phi_{s,0}$) and the bubble size from image analysis (d_n) in the following relationship:

$$\phi_{s,0} = \frac{\pi}{6} \times d_n^3 \times N_s. \tag{4}$$

Figure 4a shows the observed foam-volume growth using *PARAPOL* 1300 at 2.12 wt. % initial volatile concentration [P_{g0} = 60 psig (515 kPa)]. It is clear that foaming occurs very quickly in the first minute. A constant maximum foam-volume change was observed and was found to be approximately a 7.5 increase in volume expansion. Foam collapse was also observed in the experiments. As expected, experimental condition Run 2 with more smaller nitrogen bubbles (N_S = 1,593 No./cm^3 liq., d_n = 0.076 cm) resulted in a faster rate of bubble growth and foaming. The qualitative trend that the faster the rate of foaming (Run 2), the sooner the foam collapse occurred (2 min), was observed. In Run 3 (N_s = 33 No./cm^3 liq., d_n = 0.18 cm), however, foam collapse occurred after 5 min.

Figure 5a shows the observed foam-volume growth using *PARAPOL* 1300 at 1.27 wt. % initial volatile concentration [P_{g0} = 30 psig (308 kPa)]. Similarly, bubble growth and foaming occur very quickly in the beginning. The maximum foam-volume change was roughly a 6.5 to 7.5 expansion, except in experimental condition Run 2 (N_s = 1,175 No./cm^3 liq., d_n = 0.071 cm), which showed a significantly higher rate of foaming and foam-volume growth (8.5 expansion) than the other conditions. Furthermore, the volatile concentration showed little ability to limit the rate of foaming and the maximum extent of foam growth. However, the volatile concentration may have some effect on the duration of the foaming process.

In the experiments with *INDOPOL* H300, the maximum foam-volume growth was seen to decrease primarily because of the increase in polybutene viscosity. Figures 6a and 7a show the observed foam-volume growth using *INDOPOL* H300 at 1.66 wt. % and 0.99 wt. % initial volatile concentrations [P_{g0} = 60 psig (515 kPa) and 30 psig (308 kPa)], respectively. The rate of foaming was also decreased due to viscosity limitation. It took longer (more than 3 min) for the polymer to foam and break. The initial volatile concentration showed no effect on limiting the maximum foam-volume growth. The maximum foam-volume change was mostly in the range of 3.5 to 5 times expansion.

In the experiments with *PARAPOL* 2400, dispersion of a

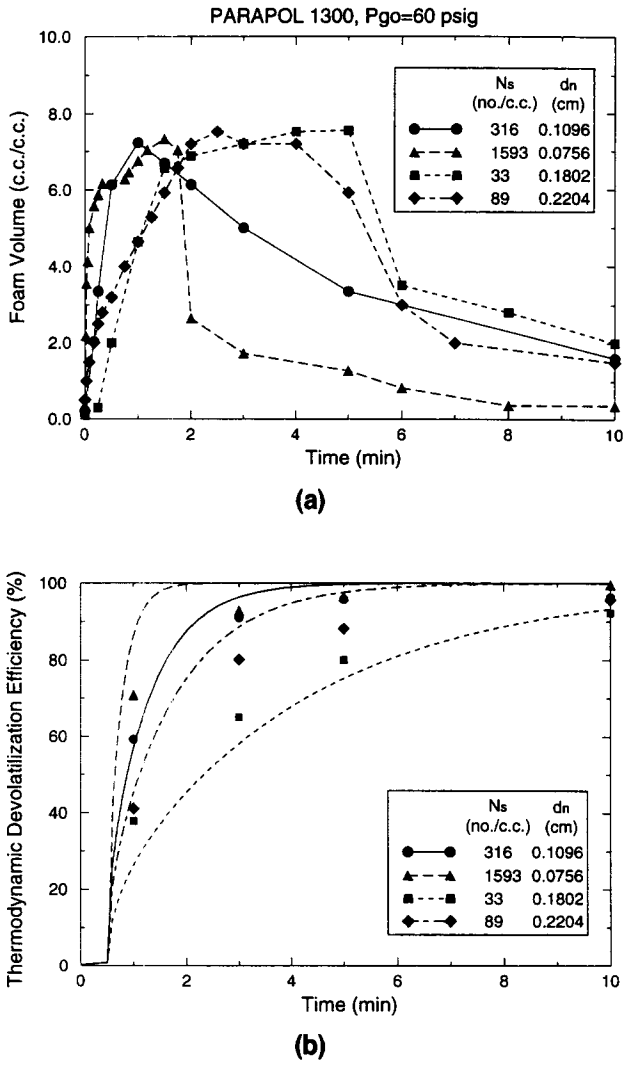

Figure 4. *PARAPOL* 1300, $C_0 = 2.12$ wt. % [$P_{g0} = 60$ psig (515 kPa)]: (a) foam volume vs. time; (b) thermodynamic devolatilization efficiency vs. time.

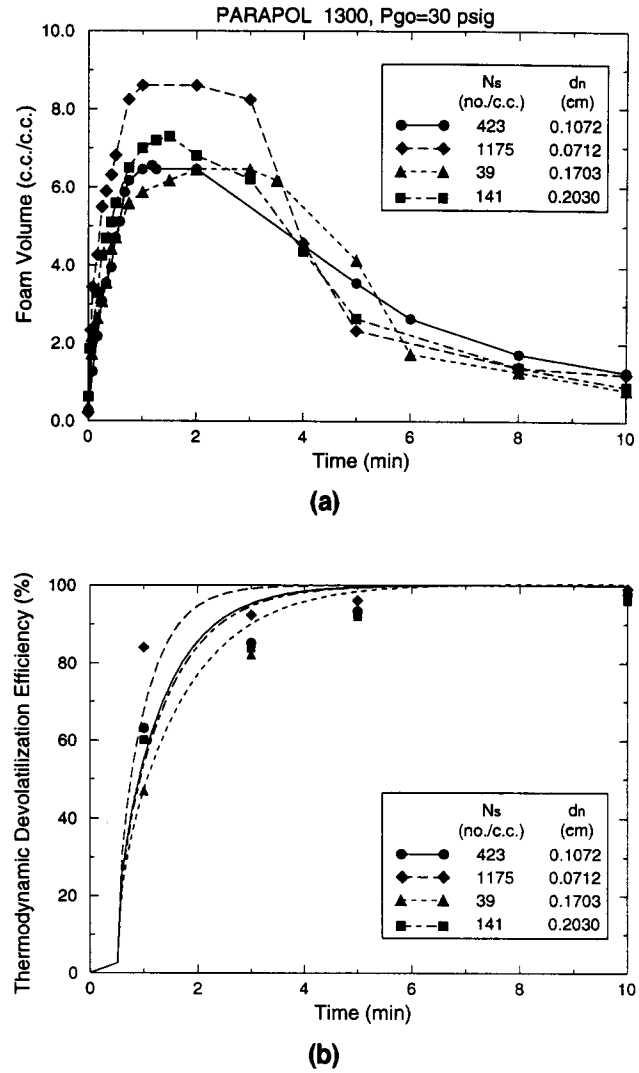

Figure 5. *PARAPOL* H1300, $C_0 = 1.27$ wt. % [$P_{g0} = 30$ psig (308 kPa)]: (a) foam volume vs. time; (b) thermodynamic devolatilization efficiency vs. time.

large number of nitrogen bubbles is difficult due to the high polymer viscosity ($\eta = 200$ Pa·s). Furthermore, the sizes of the dispersed nitrogen bubbles are also larger than those dispersed when using *PARAPOL* 1300 ($\eta = 60$ Pa·s) and *INDOPOL* H300 ($\eta = 90$ Pa·s). Figure 8a shows the observed foam-volume growth using *PARAPOL* 2400 at 1.21 wt. % initial volatile concentration ($P_{g0} = 60$ psig). Bubble growth was observed when the polymer was exposed to a vacuum. However, it required a longer period of time to observe foaming, if any. In addition, the rate of bubble growth and the extent of foam-volume change were apparently limited by the high viscosity of the polymer surrounding the bubbles. The maximum foam-volume change was only about one- to twofold expansion. This behavior may be partly due to the low number of initially dispersed nitrogen bubbles in the polymer pool.

Figure 9a shows the observed foam-volume growth using *PARAPOL* 2400 at 0.72 wt. % initial volatile concentration [$P_{g0} = 30$ psig (308 kPa)]. Under these circumstances, the rate of bubble growth was slow and the maximum foam growth was limited by the high polymer viscosity. The maximum foam-volume change was found to be a one-and-half-to threefold expansion. The effects of the number of dispersed nitrogen bubbles and the volatile concentration merely play secondary roles. Comparing the foam-volume change (7.5) in Run 3 of *PARAPOL* 1300 at 60 psig (515 kPa) ($N_s = 33$ No./cm^3 liq., $d_n = 0.18$ cm) with the 2.5 foam-volume expansion in Run 3 of *PARAPOL* 2400 and 30 psig (308 kPa) ($N_s = 31$ No./cm^3 liq., $d_n = 0.17$ cm) suggests that in some cases the number and size of nitrogen bubbles show little or no effect on the maximum foam-volume expansion within the experimental conditions investigated. Furthermore, the comparison shows, at least qualitatively, that a roughly threefold increase in polybutene viscosity from 60 to 200 Pa·s results in a decrease in the maximum foam-volume change from a 7.5 to 2.5 expansion, while increasing viscosity by one-and-half-fold from 60 to 90 Pa·s decreases the maximum foam volume from 7.5 to 4.5 times.

Figure 10 graphically shows the effect of various factors on the maximum foam volume. Viscosity seems to show a sec-

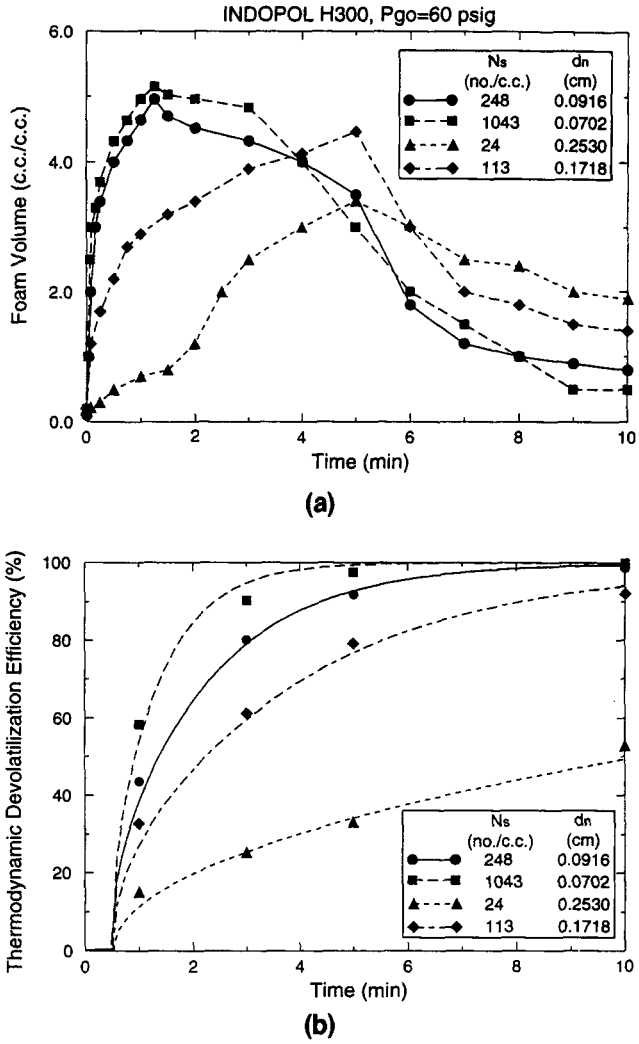

Figure 6. *INDOPOL* H300, $C_0 = 1.66$ wt. % [$P_{g0} = 60$ psig (515 kPa)]: (a) foam volume vs. time; (b) thermodynamic devolatilization efficiency vs. time.

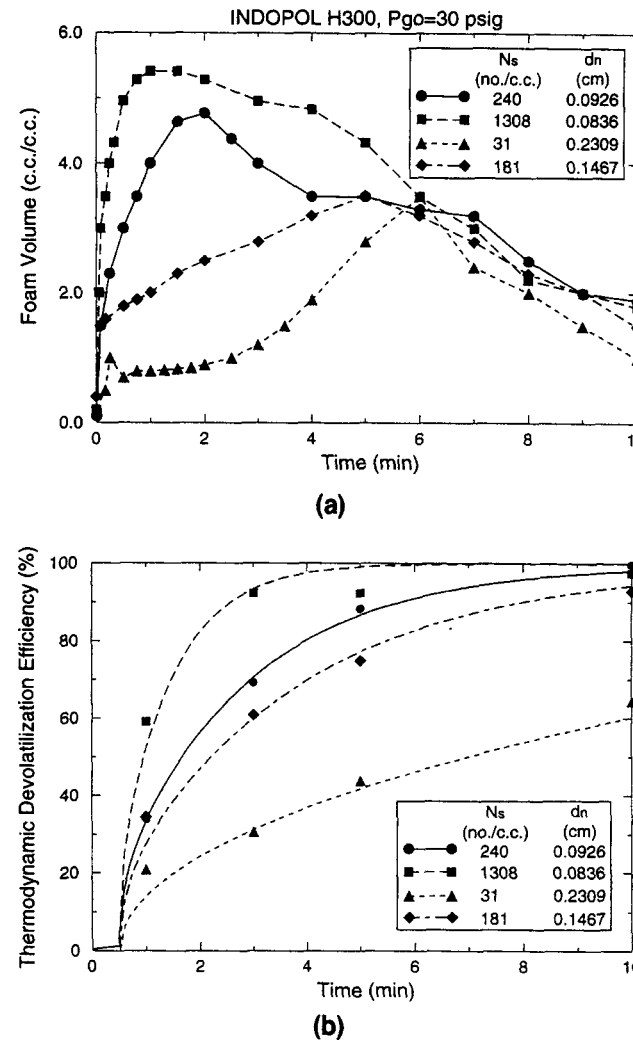

Figure 7. *INDOPOL* H300, $C_0 = 0.99$ wt. % [$P_{g0} = 30$ psig (308 kPa)]: (a) foam volume vs. time; (b) thermodynamic devolatilization efficiency vs. time.

ond-order quadratic correlation with maximum foam volume ($R^2 = 0.9154$), which is a better fit than a linear regression ($R = -0.8919$; $R^2 = 0.7955$). The number of bubbles shows a positive linear effect on the maximum foam volume ($R = 0.4980$; $R^2 = 0.2480$), though the data are somewhat scattered. As expected, bubble size has a negative linear effect on the maximum foam volume ($R = -0.4990$; $R^2 = 0.2490$). The initial volatile concentration has no effect on the maximum foam volume ($R = 0.0029$; $R^2 = 0.0000$), which is in agreement with the results in the previous foaming experiments (Yang, 1995; Yang et al., 1996a,b, 1997). In other words, the conditions for foaming are determined more by the creation of bubbles in the polymer than by the volatile concentration and are strongly limited by the viscosity of the polymer.

Comparison of Model with Experiments

Thermodynamic devolatilization efficiency calculated by the bimodal/film model is compared with that obtained from the polybutene foaming experiments. Thermodynamic devolatilization efficiency (TDE) obtained from experiments is defined as the actual amount of carbon dioxide devolatilized (ΔC_{actual}) relative to the theoretical degree of supersaturation between the initial saturation pressure and the operating vacuum pressure ($C_0 - C_e$), all in cm^3 at STP/cm^3. It can be expressed in the following equation:

$$\text{TDE}\% = \frac{\Delta C_{\text{actual}}}{C_0 - C_e} \times 100\%, \tag{5}$$

where

$$C_0 = S \times P_0 \tag{6}$$

$$C_e = S \times P_{\text{vac}}. \tag{7}$$

Carbon dioxide concentrations can also be calculated using the Henry's law and expressed in weight fractions:

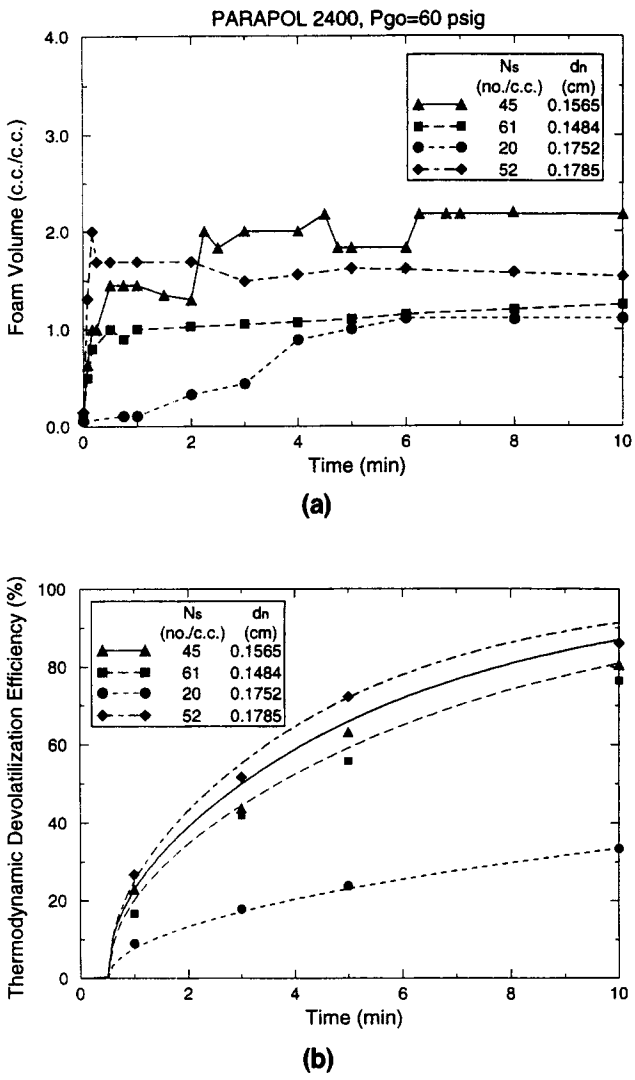

Figure 8. *PARAPOL* 2400, $C_0 = 1.21$ wt. % [$P_{g0} = 60$ psig (515 kPa)]: (a) foam volume vs. time; (b) thermodynamic devolatilization efficiency vs. time.

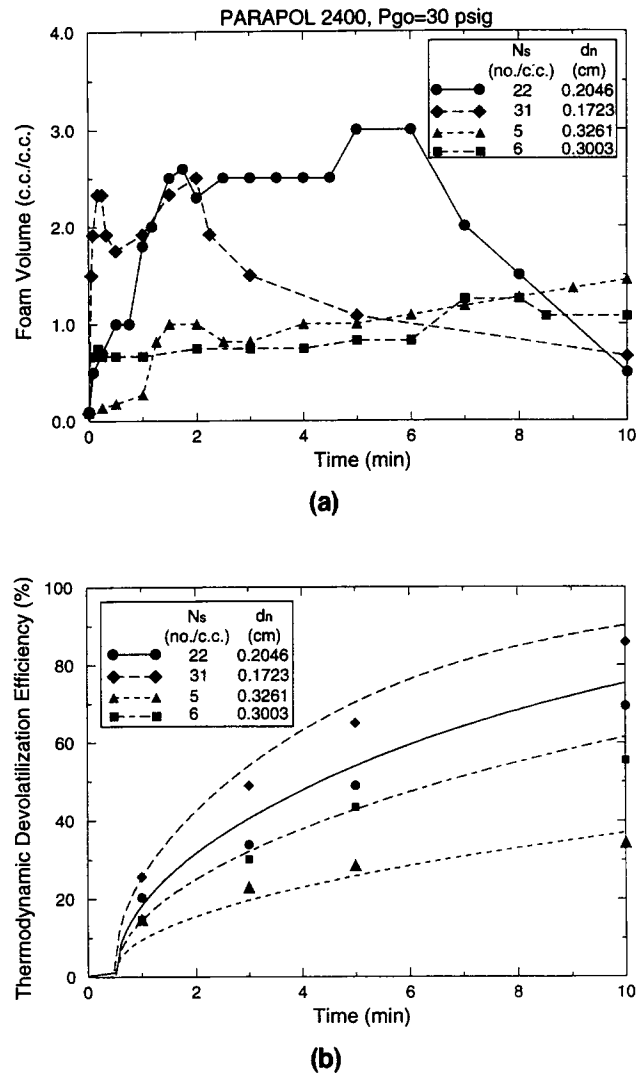

Figure 9. *PARAPOL* 2400, $C_0 = 0.72$ wt. % [$P_{g0} = 30$ psig (308 kPa)]: (a) foam volume vs. time; (b) thermodynamic devolatilization efficiency vs. time.

$$P = H_w \times C \tag{8}$$

As observed in the experiments, maximum foam-volume expansions mostly occurred after 1 min. Carbon dioxide was collected at 0–1, 1–3, 3–5, and 5–10 min. We expect that significant devolatilization should have occurred by the time (1 min) the foam reaches maximum expansion. In our model we have shown that the bimodal model for initial foam growth predicts a low degree of devolatilization, while the film model is used to complete the devolatilization computation. Since experimentally we take our first data after 1 min, and much of the devolatilization process has occurred in the first 30 s, we matched the foam-volume growth computed using the bimodal model with the one observed in the experiment for approximately 30 s. Then the film model was incorporated to complete the TDE calculation to 10 min.

The experimental data and model simulation in the TDE vs. time are shown in Figures 4b through 9b. Symbols represent the experimental data and lines are computed from the model. The parameters (initial number and size of stripper bubbles) in Figures 4b through 9b were determined in the stripper-dispersion experiment and were the same as those used in model computation. The model predictions show good agreement with the experimental data. The trend in the devolatilization efficiency was similar to experimental observations in the rate of foam growth and expansion, with less than a 10% error rate. In other words, the faster the rate of foaming and breakup, the higher the rate of devolatilization efficiency. The data in Figures 4b and 5b show larger deviation from the model than do Figures 6b to 9b. This may be due to the faster foaming rate, which causes more experimental error in the vacuum trapping system for condensing the volatile vapor. Considering the glass trapping system used to collect carbon dioxide and the vapor-pressure measurement, the results were relatively good.

Figure 11 shows the effect of the initial foaming rate on the final or maximum TDE in the polybutene foaming experiments. The initial foaming rate is taken as the initial slope in

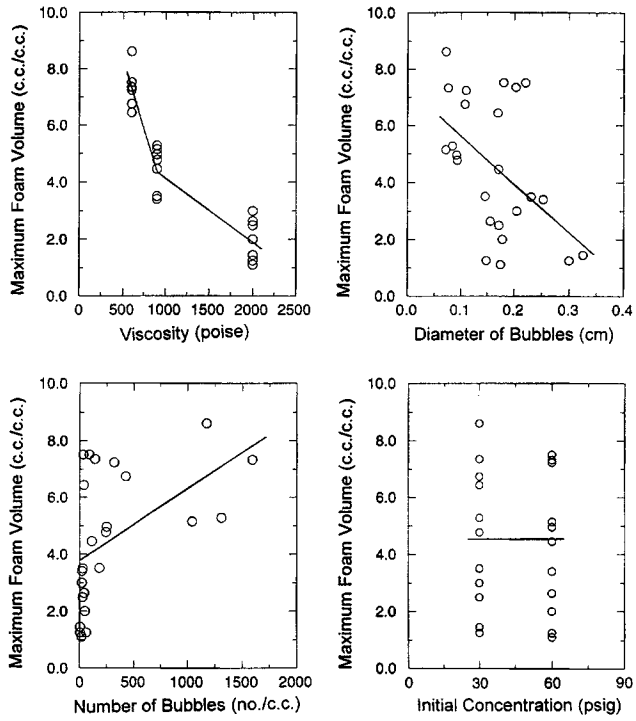

Figure 10. Effects of various factors on the maximum foam-volume expansion.

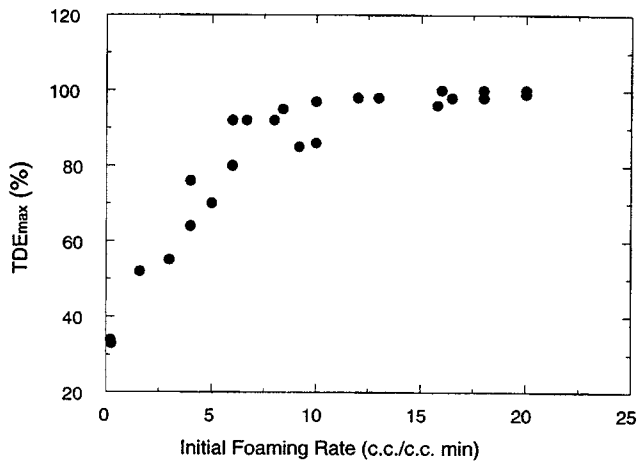

Figure 11. Effect of the initial foaming rate on the thermodynamic devolatilization efficiency.

the plot of foam volume vs. time for each experimental condition (Figures 4a to 9a). We note that there appears to be a threshold condition of the initial foaming rate in order to achieve over 90% efficiency. In this case, the initial threshold foaming rate is about 6 cm^3 gas/cm^3 liq. min. It is suggested that proper conditions be created to overcome the initial threshold foaming rate and obtain high devolatilization efficiency, such as by dispersing stripper bubbles into the polymer melt.

Conclusions

Based on a case study that uses polystyrene/styrene devolatilization in a W&P ZSK-90 corotating twin-screw extruder, we have shown the effectiveness of our model and compared it with the cell model for devolatilization in the literature. Our model has shown improvement over this cell model in two respects:

- It requires a lower initial number of bubbles, which is more physically achievable and believable.
- It accounts for the observation of a limiting foam-volume growth for a polymer pool in devolatilization.

A stripper dispersion experiment was designed to investigate the effect of the dispersed stripper bubbles on foam dynamics and devolatilization performance. Also examined were the effects of the number and size of initially dispersed nitrogen bubbles. The bubble population was determined by photography and image analyses. In the experiments with *PARAPOL* 1300 ($\eta = 60$ Pa·s), foaming and surface rupture were found to occur very quickly in the first minute. The maximum foam volume change was mostly in the 6.5- to 7.5-fold expansion range. The maximum foam-volume change for *INDOPOL* H300 ($\eta = 90$ Pa·s) was somewhat limited (between 3.5 and 5 times expansion), as polybutene viscosity increased from 60 Pa·s to 90 Pa·s. On the other hand, the foaming rate and the maximum achievable foam-volume growth were clearly limited by the high viscosity of *PARAPOL* 2400 polybutene ($\eta = 200$ Pa·s). The maximum observed foam growth was in the range of only one- to threefold volume expansion. Viscosity is the more dominant factor in limiting the rate of foam and the maximum foam-volume expansion. In some cases the number and size of nitrogen bubbles were found to have little or no effect on the maximum foam-volume change. The volatile concentration has no effect on limiting the maximum foam-volume expansion.

The bimodal model for foam growth, combined with the film model for devolatilization, was used for comparison with the experimental data. Model predictions show relatively good agreement with the experiments. The thermodynamic devolatilization efficiency closely followed the rate of foaming and surface breakup. In other words, the faster the foaming rate the more rapid the mass-transfer rate in polymer devolatilization.

Our work suggests that foam-volume expansion and time are better parameters than the initial number and size of bubbles for characterizing foam devolatilization in extruders. The initial number and size of bubbles are just fitted parameters to make the cell model and the bimodal/film model work and match with experimental data. They are difficult to observe and quantify during the foaming, which is a dynamic and complex process involving bubble formation, growth, coalescence, and breakup. On the other hand, the foam-volume expansion for a polymer is physically observable and can be used as a process parameter in operating an extruder for devolatilization.

Acknowledgments

The authors gratefully acknowledge the financial support from DuPont Central Research and Development Department, Wilmington, DE.

Notation

C = concentration, g/g
D = diffusion coefficient, cm^2/s

P = pressure, Pa
P_{vac} = vacuum pressure, mmHg
R = correlation coefficient
S = solubility, cm^3 at STP/cm^3 atm
t = time, s
w = weight fraction, g/g
δ = film thickness, cm

Subscripts

e = equilibrium
g = gas
s = stripping agent

Literature Cited

Albalak, R., Z. Tadmor, and Y. Talmon, "Scanning Electron Microscopy Studies of Polymer Melt Devolatilization," *AIChE J.*, **33,** 808 (1987).

Albalak, R. J., Z. Tadmor, and Y. Talmon, "Polymer Melt Devolatilization Mechanisms," *AIChE J.*, **36,** 1313 (1990).

Amoco, *INDOPOL Polybutene Bulletins 12-N & 12-23b*, Amoco Chemical Co., Naperville, IL (1995).

Crank, J., and G. S. Park, *Diffusion in Polymers*, Academic Press, New York (1968).

Exxon, *PARAPOL Polybutene Paramins Bulletin,* Exxon Chemical Co., NJ (1995).

Lee, S.-T., and J. A Biesenberger, "A Fundamental Study of Polymer Melt Devolatilization: IV. Some Theories and Models for Foam-Enhanced Devolatilization," *Poly. Eng. Sci.*, **29**, 782 (1989).

Newman, R. E., and R. H. M. Simon, "A Mathematical Model of Devolatilization Promoted by Bubble Formation," AIChE Meeting, Chicago (1980).

Rosen, B., "A Recording Sorption Kinetics Apparatus," *J. Poly. Sci.*, **35,** 335 (1959).

Sakakibara, Y., H. Takatori, I. Yamada, and S. Hiraoka, "Mutual Diffusivity of Volatile Materials in Molten Polystyrene," *J. Chem. Eng. Jpn.* **23,** 170 (1990).

Tukachinsky, A., Z. Tadmor, and Y. Talmon, "Ultrasound-enhanced Devolatilization of Polymer Melt," *AIChE J.*, **39,** 359 (1993).

Tukachinsky, A., Y. Talmon, and Z. Tadmor, "Foam-enhanced Devolatilization of Polystrene Melt in a Vented Extruder," *AIChE J.*, **40,** 670 (1994).

Werner, H., *Devolatilisation of Plastics*, Verein Deutscher Ingenieure VDI-GmbH, Dusseldorf (1980).

Yang, C.-T., "A Study of Trace Devolatilization of Polymers," PhD Thesis, Univ. of Maryland at College Park (1995).

Yang, C.-T., T. G. Smith, D. I. Bigio, and C. Anolick, "A Mathematical Model of Polymer Devolatilization," *SPE ANTEC Tech. Papers*, p. 350 (1996a).

Yang, C.-T., T. G. Smith, D. I. Bigio, and C. Anolick, "Polymer Trace Devolatilization: Foam Experiments and Modeling," *AIChE Meeting*, Paper 213b, Chicago (1996b).

Yang, C.-T., T. G. Smith, D. I. Bigio, and C. Anolick, "Polymer Trace Devolatilization: I. Foaming Experiments and Model Development," *AIChE J.*, **43**(7), 1861 (July, 1997).

Manuscript received Apr. 22, 1996, and revision received Mar. 3, 1997.